nature protocols

PROTOCOL

https://doi.org/10.1038/s41596-022-00762-y

Check for updates

Fabrication of liquid cell for in situ transmission electron microscopy of electrochemical processes

Ruijie Yang[1], Liang Mei[1], Yingying Fan[1], Qingyong Zhang[1], Hong-Gang Liao[2], Juan Yang[3], Ju Li[4]✉ and Zhiyuan Zeng[1,5]✉

Fundamentally understanding the complex electrochemical reactions that are associated with energy devices (e.g., rechargeable batteries, fuel cells and electrolyzers) has attracted worldwide attention. In situ liquid cell transmission electron microscopy (TEM) offers opportunities to directly observe and analyze in-liquid specimens without the need for freezing or drying, which opens up a door for visualizing these complex electrochemical reactions at the nano scale in real time. The key to the success of this technique lies in the design and fabrication of electrochemical liquid cells with thin but strong imaging windows. This protocol describes the detailed procedures of our established technique for the fabrication of such electrochemical liquid cells (~110 h). In addition, the protocol for the in situ TEM observation of electrochemical reactions by using the nanofabricated electrochemical liquid cell is also presented (2 h). We also show and analyze experimental results relating to the electrochemical reactions captured. We believe that this protocol will shed light on strategies for fabricating high-quality TEM liquid cells for probing dynamic electrochemical reactions in high resolution, providing a powerful research tool. This protocol requires access to a clean room equipped with specialized nanofabrication setups as well as TEM characterization equipment.

Introduction

Transmission electron microscopy (TEM) is a sophisticated sub-nanometer-resolution imaging technology that plays a central role in today's life sciences, material sciences, physics and chemistry[1]. This technology is constantly evolving, offering rich and direct structural and compositional information at atomic-level resolution[1]. However, the use of conventional TEM, with carbon films on copper grids as the sample carrier, is limited to thin, stable and solid samples because of the vacuum environment of the chamber[2–5]. Liquid specimens, particularly high-equilibrium vapor pressure ones, are vacuum incompatible and therefore cannot be directly probed in traditional TEM.

TEM with a 'closed' liquid cell opens up the possibility of directly observing and analyzing liquid specimens without the need for freezing or drying processes[2,6–11]. Such a 'closed' liquid cell mainly fulfills two functions: (i) enclosing the liquid samples in a closed container, thereby separating them from the microscope vacuum environment; and (ii) confining the liquid samples into a liquid layer by using two electron-transparent silicon nitride (SiN_x) windows, thin enough so that electrons can travel through the liquid layer and image the reactions. The emergence of this technology offers the opportunity for the in situ study of important liquid-phase processes, including crystal nucleation and growth in solution[12–19], electrochemical reactions in energy devices[20–33] and the biological activities of cells in their native state (such as cell division)[34,35], to name but a few[6,36].

Development of an electrochemical liquid cell

Incorporating electrodes that are patterned by photolithography into a regular 'closed' liquid cell, named an 'electrochemical liquid cell', opens up the door for directly observing electrochemical reactions in real time. The fabrication of electrochemical liquid cells has only a short history of fewer

[1]Department of Materials Science and Engineering, City University of Hong Kong, Kowloon, Hong Kong, China. [2]State Key Lab of Physical Chemistry of Solid Surfaces, College of Chemistry and Chemical Engineering, Xiamen University, Xiamen, China. [3]School of Chemical Engineering and Technology, Xi'an Jiaotong University, Xi'an, China. [4]Department of Nuclear Science and Engineering and Department of Materials Science and Engineering, Massachusetts Institute of Technology, Cambridge, MA, USA. [5]Shenzhen Research Institute, City University of Hong Kong, Shenzhen, China. ✉e-mail: liju@mit.edu; zhiyzeng@cityu.edu.hk

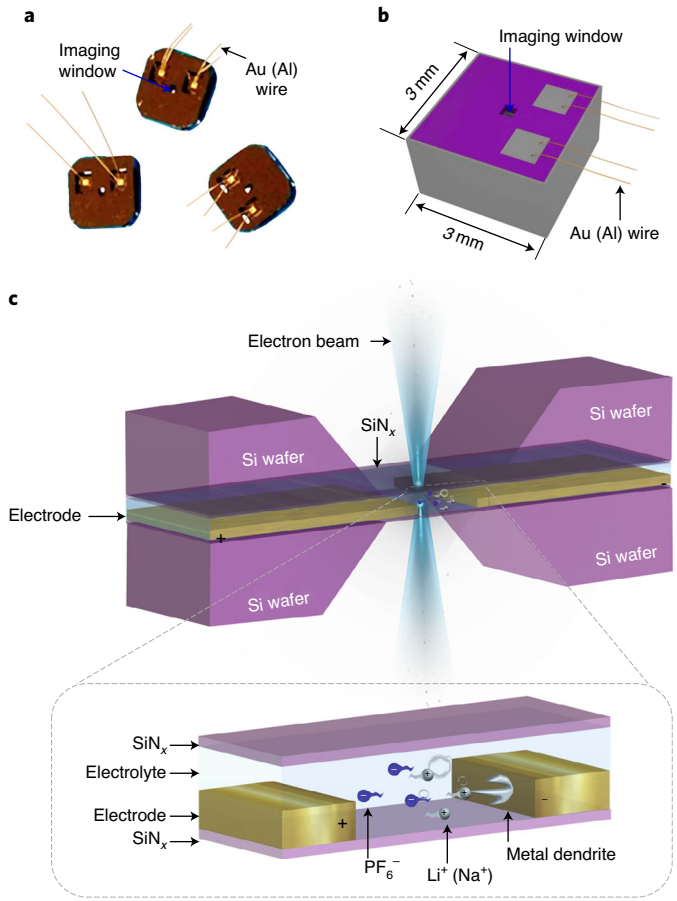

Fig. 1 | Electrochemistry liquid cell (E-cell) fabricated by this protocol. a, Photographs of the E-cells (3 mm × 3 mm). **b**, Schematic illustration of the E-cell. The wafer is purple, and the epoxy is gray. **c**, Section view of the E-cell at the imaging window, showing the internal composition and structure of the E-cell. From top to bottom, its constituent elements are as follows: silicon wafer, SiN_x, electrolyte, electrode, SiN_x and silicon wafer in turn. The bottom panel shows an enlarged view of the region illuminated by the electron beam, illustrating the electrochemical reaction (e.g., formation of metal dendrite) to be observed.

than 20 years. In 2003, Ross et al.[20] first fabricated an electrochemical liquid cell with a SiN_x film (80-nm thick) on a silicon substrate as the observation window, and the deposited polycrystalline gold as the working electrode. This creatively allowed the in situ observation of the nucleation and growth of nanoscale copper clusters during the electrodeposition process. In 2009, Zheng et al. further developed this technology by reducing the thickness of the SiN_x window film down to 25 nm without incorporating gold electrodes, thereby improving the imaging resolution[12]. With continued development, the liquid cell products produced through this technique have now been commercialized by several manufacturers (e.g., Hummingbird Scientific, Protochips, DENSsolutions and Zeptools)[28]. However, the TEM resolution based on these commercial liquid cells is unsatisfactory because of the thick SiN_x windows (~100 nm), as well as the thick liquid layer (0.5–1.0 μm). Beyond SiN_x, graphene has also been demonstrated as an alternative window material for liquid cells by Yuk et al.[13,37]. The thin nature of the graphene window allows a high resolution for such liquid cell TEM. However, integrating electrodes into graphene liquid cells is difficult.

Recently, Liao et al. developed a regular liquid cell with a SiN_x window thickness down to 15 nm and liquid layer thickness down to 0.12 μm, which greatly improved the TEM resolution to the atomic level for movie capturing[15]. On this basis, we further used this technique to fabricate an electrochemical liquid cell (Fig. 1), by incorporating gold or titanium electrodes into the regular liquid cells. Owing to the integration of patterned electrodes, the thickness of the SiN_x window was readjusted to 35 nm because of the different thermal expansion coefficients of SiN_x and gold (titanium) electrodes during the nanofabrication process. The procedures for the fabrication of such electrochemical liquid cells by using photolithography are detailed in this protocol.

Advantages and limitations

The electrochemical liquid cell designed by our customized nanofabrication method possesses thinner SiN_x imaging windows (35 nm) than commercial ones (50 nm). It also possesses a thinner liquid layer (150 nm) created by a thin indium spacer in contrast to that of commercial products (1,000 nm) created by an O-ring. The thinner SiN_x imaging windows and thinner liquid layer ensure that our fabricated liquid cell can capture electrochemical reactions with better TEM spatial resolution than the commercial ones (Supplementary Fig. 1). Note that the SiN_x imaging window of our liquid cell is only 35-nm thick (50-nm thick for commercial liquid cells), so it is the most vulnerable part of the entire liquid cell. However, the smaller the size of the window, the greater the mechanical strength of the liquid cell and the less likely it is to be damaged. Therefore, the smaller imaging window size (25 μm × 6 μm) and liquid reservoir size (700 μm × 500 μm) of our fabricated liquid cell guarantee a greater mechanical strength than commercial liquid cells.

Of course, there are also some limitations to our electrochemical liquid cell design. First, the indium spacer has poor acid resistance, leading to its inapplicability to encapsulate some acidic electrolytes (metals are easily corroded by acids). Second, the fabricated electrochemical liquid cell is sealed by the half-melted and resolidified indium spacer, as well as an epoxy that is also used to further ensure good sealing. Although this sealing method can ensure that the electrochemical liquid cell is well sealed and avoid electrolyte leakage, the produced liquid cell cannot be reused. This increases the fabrication cost. In addition, this protocol uses a two-electrode system in the fabricated electrochemical liquid cell, leading to its inapplicability for in situ TEM observation of electrochemical reactions in a three-electrode system. Nevertheless, an electrochemical liquid cell with a three-electrode system can be fabricated by slightly modifying this protocol. Of note, the mechanical strength of the three-electrode electrochemical liquid cell decreases in comparison with a two-electrode electrochemical liquid cell. As a result, the image resolution and successful rate of in situ TEM experiments are lower than two-electrode electrochemical liquid cells. For convenience of comparison, we summarize the advantages and limitations of two commercially developed electrochemical liquid cells and our products in Supplementary Table 1.

Applications

Our nanofabricated liquid cell has attracted attention from both academia and industry. The fabricated electrochemical liquid cell has been widely used in in situ TEM observation of various electrochemical reactions, such as lithium dendritic growth and solid electrolyte interface (SEI) formation[22], electrochemical alloying and de-alloying of gold anodes[24], electrochemical lithiation and delithiation of molybdenum disulfide nanosheets[23], sodium electrodeposition on a titanium electrode[25], lithium fluoride nanosheet formation on positively charged titanium electrodes[26] and lithium dendrite suppression by modifying solid-electrolyte interphase by using a poly(diallyldimethylammonium chloride) cationic polymer film[33]. We expect that a plethora of further opportunities and applications for in situ TEM observation of electrochemical reactions beyond those listed above will emerge in the near future. This will require the development of the electrochemical liquid cell with the selection of patterned metal electrodes and the encapsulated liquid electrolytes in the liquid cell. In addition, our fabrication protocol can be used in other in situ techniques beyond TEM. For example, with appropriate adjustment, this protocol will be suitable for the fabrication of an electrochemical liquid cell for in situ X-ray characterizations of electrochemical reactions (e.g., X-ray absorption spectroscopy and X-ray diffraction).

Experimental design

Overview of the procedure

The 'closed' electrochemical liquid cell in this protocol consists of a bottom and top chip, which are fabricated via photolithography. This involves the individual fabrication of the bottom chip and the top chip, followed by an assembly process (Fig. 2 and Supplementary Video 1).

The fabrication procedure for each of the two chips is divided into five stages: substrate preparation (Steps 1–8), the first lithography (Steps 9–17), etching (Steps 18–31), the second lithography (Steps 32–36) and metal deposition (Steps 37–42). Crucially, these Steps (1–42) are wafer-level operations. Each silicon wafer (with diameter of ~100 mm) can eventually produce hundreds of top or bottom chips (3 × 3 mm).The assembly process includes bonding together of the two chips (Steps 43–50), wire bonding (Step 51), loading electrolyte (Step 52), sealing (Steps 53–55) and

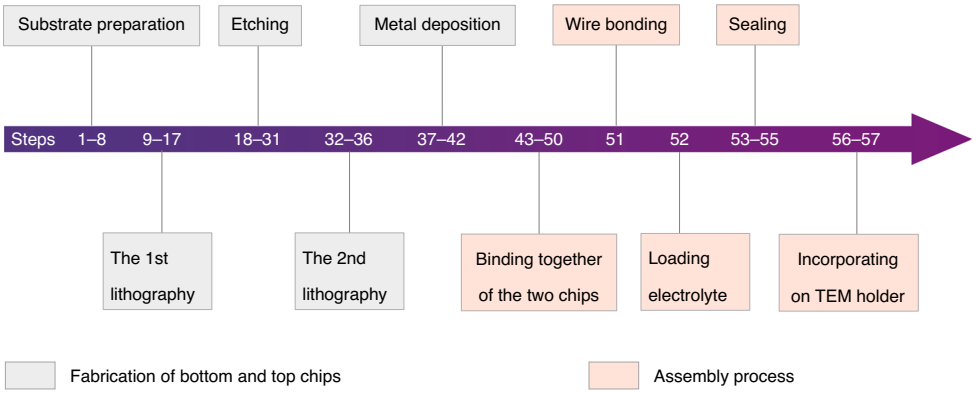

Fig. 2 | Flow chart of the fabrication of an electrochemical liquid cell in this protocol. The whole fabrication procedure includes the following: substrate preparation (Steps 1–8), the first lithography (Steps 9–17), etching (Steps 18–31), the second lithography (Steps 32–36), metal deposition (Steps 37–42), binding together of the two chips (Steps 43–50), wire bonding (Step 51), loading electrolyte (Step 52), sealing (Steps 53–55) and incorporating the cell in the TEM holder (Steps 56 and 57).

incorporating the cell in the TEM holder (Steps 56 and 57). We also briefly outline procedures for TEM observation and post in situ characterizations (Steps 58–60).

Substrate preparation (Steps 1–8)

The substrate of both the top and bottom chip consists of a silicon wafer (200-μm think, 4 inches, p-doped) to both sides of which are deposited SiN_x films (35-nm thick). The substrate preparation is carried out in a tube furnace via a low-pressure chemical vapor deposition (LPCVD) method, during which the ultrathin SiN_x membrane is evaporated onto both sides of the silicon wafer (Fig. 3a,b and Fig. 4a,b).

Lithograph and etching (Steps 9–36)

The prepared SiN_x/silicon substrate is then lithographically patterned with targeted masks and etched in turn with fluoroform (CHF_3) + oxygen (O_2) plasma followed by potassium hydroxide solution (Fig. 3c–j and Fig. 4c–j). Different masks are used for the top and bottom chips such that after these processes, an imaging window (25 μm × 6 μm) and two reservoirs (700 μm × 500 μm) are created for the top chip (Fig. 3j, left), whereas only one imaging window is created for the bottom chip (Fig. 3j, right).

Metal deposition (Steps 37–42)

In the next stage, the target metals are incorporated onto the patterned SiN_x/silicon wafer via a physical vapor deposition (PVD) method (Fig. 3k–q and Fig. 4k–q). During this process, either two gold or two titanium electrodes (90–120-nm thick) are deposited on the bottom chip with a face-to-face distance (i.e., the gap between the electrodes) of 20 μm; one of the electrodes will be the working electrode, and the other will be the counter electrode (top in Figs. 3q and 4q). Both of these two electrodes are extended to two gold (or titanium) pads in two reservoirs (top in Figs. 3q and 4q). In parallel, the indium spacer (150-nm thick) is sputtered on the top chip, working as the spacer in the assembled liquid cell (bottom in Figs. 3q and 4q). Note that the choice of the electrode (gold or titanium or others) depends on the purpose of the cell; for example, if the cell is used for probing dynamic electrochemical reactions happening on the gold electrode, then the gold electrode is chosen here; if other active material (such as MoS_2) is tested, then the titanium electrode is chosen, because the titanium electrode is inert in lithim/sodium ion battery electrolyte and can serve as a good current collector.

Assembly

Bonding together of the top and bottom chip (Steps 43–50). The preliminary liquid cell is assembled by aligning the bottom and top chips under an optical microscope (Figs. 3r and 4r). Subsequently, to increase the bonding force between the top chip and bottom chip, the preliminary liquid cell is then fixed between two glass slides clamped by two binder clips and is heated in a 120 °C oven for 2 h. This heat treatment binds the bottom and top chips together by a half melting and re-solidification of the

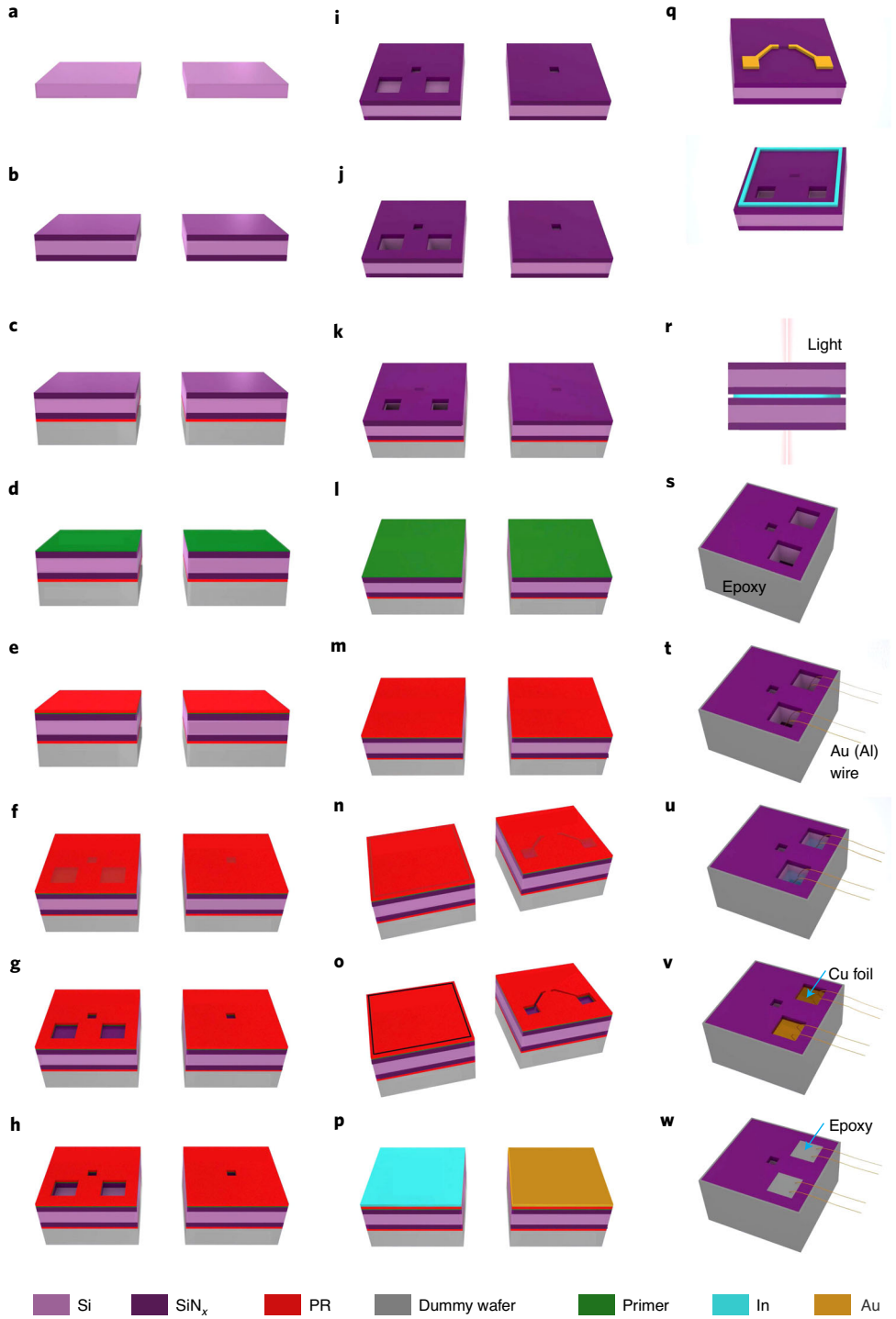

Fig. 3 | Evolution of the E-cell during the fabrication process. Schematics **a**–**p** show the top chip on the left and the bottom chip on the right. **a**, The silicon wafer after a pre-furnace clean (after Step 3). **b**, The silicon wafer after low-stress SiN_x growth (after Step 5). **c**, The wafer after bonding the SiN_x/silicon wafer on a dummy wafer (after Step 8). **d**, The wafer after the first primer coating (after Step 10). **e**, The wafer after the first photoresist coating (after Step 12). **f**, The wafer after the first UV exposure (Step 15). **g**, The wafer after the first photoresist development (after Step 17). **h**, The wafer after plasma etching (after Step 23). **i**, The wafer after the first liftoff (after Step 26). **j**, The wafer after wet etching (after Step 31). **k**, The wafer after flip-over and bonding (after Step 32). **l**, The wafer after the second primer coating (after Step 33). **m**, The wafer after the second photoresist coating (after Step 34). **n**, The wafer after the second UV exposure (after Step 35). **o**, The wafer after the second photoresist development (after Step 36). **p**, The wafer after metal deposition (after Step 38). **q**, The completed bottom chip and top chip (after Step 42). **r**, The liquid cell during assembly of the top chip and bottom chip (after Step 46). **s**, The liquid cell after evenly coating epoxy all around the sides of the liquid cell (after Step 50). **t**, The liquid cell after wire bonding (after Step 51). **u**, The liquid cell after loading electrolyte (after Step 52). **v**, The liquid cell after putting two copper foils on the two reservoirs (after Step 53). **w**, The liquid cell after epoxy coating the top reservoir areas (after Step 54). PR, photoresist.

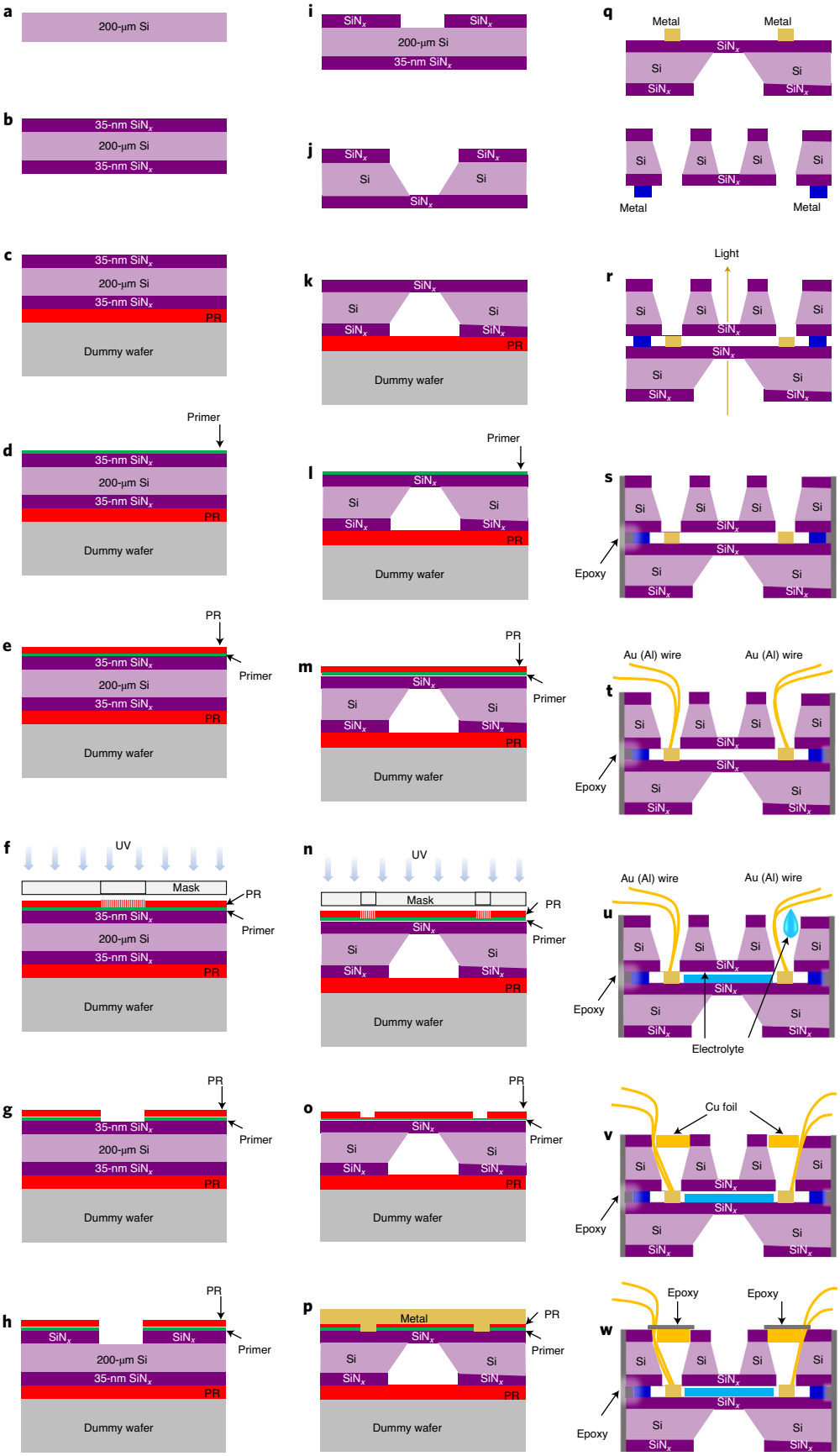
a
200-μm Si
b
35-nm SiNx
200-μm Si
35-nm SiNx
c
35-nm SiNx
200-μm Si
35-nm SiNx
PR
Dummy wafer
d
Primer
35-nm SiNx
200-μm Si
35-nm SiNx
PR
Dummy wafer
e
PR
Primer
35-nm SiNx
200-μm Si
35-nm SiNx
PR
Dummy wafer
f
UV
Mask
PR
Primer
35-nm SiNx
200-μm Si
35-nm SiNx
PR
Dummy wafer
g
PR
Primer
35-nm SiNx
200-μm Si
35-nm SiNx
PR
Dummy wafer
h
PR
Primer
SiNx
SiNx
200-μm Si
35-nm SiNx
PR
Dummy wafer
i
SiNx
SiNx
200-μm Si
35-nm SiNx
j
SiNx
SiNx
Si
Si
SiNx
k
SiNx
Si
Si
SiNx
SiNx
PR
Dummy wafer
l
Primer
SiNx
Si
Si
SiNx
SiNx
PR
Dummy wafer
m
PR
Primer
SiNx
Si
Si
SiNx
SiNx
PR
Dummy wafer
n
UV
Mask
PR
Primer
SiNx
Si
Si
SiNx
SiNx
PR
Dummy wafer
o
PR
Primer
SiNx
Si
Si
SiNx
SiNx
PR
Dummy wafer
p
Metal
PR
Primer
SiNx
Si
Si
SiNx
SiNx
PR
Dummy wafer
q
Metal
Metal
SiNx
Si
Si
SiNx
SiNx
Si
Si
Si
Si
SiNx
Metal
Metal
r
Light
Si
Si
Si
Si
SiNx
SiNx
Si
Si
SiNx
SiNx
s
Si
Si
Si
Si
SiNx
SiNx
Epoxy
Si
Si
SiNx
SiNx
t
Au (Al) wire
Au (Al) wire
Si
Si
Si
Si
SiNx
SiNx
Epoxy
Si
Si
SiNx
SiNx
u
Au (Al) wire
Au (Al) wire
Si
Si
Si
Si
SiNx
SiNx
Epoxy
Si
Si
SiNx
SiNx
Electrolyte
v
Cu foil
Si
Si
Si
Si
SiNx
SiNx
Epoxy
Si
Si
SiNx
SiNx
w
Epoxy
Epoxy
Si
Si
Si
Si
SiNx
SiNx
Epoxy
Si
Si
SiNx
SiNx

◀ **Fig. 4 | Schematic illustration of the wafer cross-section at different fabrication stages.** Because of the similarity of the top chip with the bottom chip, panels **a–p** show only the side view of one of them (bottom chip). **a**, Cross-section of the silicon wafer after a pre-furnace clean (after Step 3). **b**, Cross-section of the silicon wafer after low-stress SiN_x growth (after Step 5). **c**, Cross-section of the wafer after bonding the SiN_x/silicon wafer on a dummy wafer (after Step 8). **d**, Cross-section of the wafer after the first primer coating (after Step 10). **e**, Cross-section of the wafer after the first photoresist coating (after Step 12). **f**, Cross-section of the wafer during the first UV exposure (Step 14). **g**, Cross-section of the wafer after the first photoresist development (after Step 17). **h**, Cross-section of the wafer after plasma etching (after Step 23). **i**, Cross-section of the wafer after the first liftoff (after Step 26). **j**, Cross-section of the wafer after wet etching (after Step 31). **k**, Cross-section of the wafer after flip-over and bonding (after Step 32). **l**, Cross-section of the wafer after the second primer coating (after Step 33). **m**, Cross-section of the wafer after the second photoresist coating (after Step 34). **n**, Cross-section of the wafer during the second UV exposure (Step 35). **o**, Cross-section of the wafer after the second photoresist development (after Step 36). **p**, Cross-section of the wafer after metal deposition (after Step 38). **q**, Cross-section of the completed bottom chip and top chip (after Step 42). **r**, Cross-section of the liquid cell after assembly of the top chip and bottom chip (after Step 46). **s**, Cross-section of the liquid cell after evenly coating epoxy all around the sides of the liquid cell (after Step 50). **t**, Cross-section of the liquid cell after wire bonding (after Step 51). **u**, Cross-section of the liquid cell after loading electrolyte (after Step 52). **v**, Cross-section of the liquid cell after putting two copper foils over the two reservoirs (after Step 53). **w**, Cross-section of the liquid cell after epoxy coating the top reservoir areas (after Step 54).

indium spacer. To enhance the bonding between the top chip and the bottom chip, as well as to prevent leakage, epoxy is evenly coated all around the sides of the liquid cell (Figs. 3s and 4s).

Wire bonding (Step 51). Subsequently, gold (aluminum) wires are bonded onto each gold (titanium) pad in the two reservoirs (Figs. 3t and 4t). Note that gold wires are used to bond a gold pad, and aluminum wires are used for a titanium pad. The wire bonding process uses a wire bonder, which is operated under an optical microscope.

Electrolyte loading (Step 52). Liquid electrolyte is then loaded into the reservoir by using a syringe with a Teflon tube. After loading of liquid electrolyte into the reservoir, the liquid electrolyte will spread out quickly in the entire space of the liquid cell by capillary force (Figs. 3u and 4u). Note that the choice of electrolyte also depends on the purpose of the cell; for instance, if the cell is used for probing dynamic electrochemical reactions of a lithium-ion battery, then an electrolyte containing lithium ions is chosen, such as 1 M $LiPF_6$ dissolved in 1:1 (vol/vol) ethylene carbonate (EC) and diethyl carbonate (DEC); if the cell is used for probing dynamic electrochemical reactions of a sodium-ion battery, then an electrolyte containing sodium ions is chosen, such as 1 M $NaPF_6$ dissolved in propylene carbonate (PC).

Sealing (Steps 53–55). The electrochemistry liquid cell is completed by sealing two reservoirs of the cell by using copper foil (Figs. 3v and 4v) and epoxy (Figs. 3w and 4w). Note that the function of the copper foil is to cover the reservoirs (epoxy further seals the contact edges between the copper foil and reservoir) so as to minimize the direct contact between the electrolyte and epoxy and to prevent the electrolyte from leaking out of the reservoirs. Alternatively, other thin foils, such as aluminum or titanium foil can also be used, as long as they do not react with the liquid electrolyte.

Incorporating the cell into the TEM holder (Steps 56 and 57). Once the liquid cell is placed in the cell pocket of the holder tip, the gold (aluminum) wires extending from the liquid cell are located and soldered onto the two copper pads in the holder tip. After that, the screw of the liquid cell retainer is tightened to fix its position.

TEM observation and post in situ characterizations (Steps 58–60)

The next stages are the in situ TEM observation of the electrochemical reactions (Steps 58 and 59) and the post in situ characterizations (Step 60). For in situ TEM observation, the TEM holder is inserted into the TEM instrument and connected to the electrochemical workstation. When the electrochemical program output by the electrochemical workstation is applied to the tiny electrochemical liquid cell through the wires connected to the TEM holder, the dynamic electrochemical reactions on the electrode surface will be recorded in real time with high resolution through the TEM operation system incorporated with a high-spatiotemporal-resolution camera.

After the dynamic electrochemical reaction in the liquid cell is captured by TEM and the cyclic voltammetry (or other electrochemical techniques) is stopped, the post in situ characterizations (in other words, ex situ TEM characterizations) are carried out. Techniques such as high-angle annular dark field-scanning transmission electron microscopy (HAADF-STEM), energy dispersive spectroscopy (EDS) and 4D scanning transmission electron microscopy (4D-STEM) (nanodiffraction dataset) are conducted to obtain the Z-contrast image, elemental composition map and crystal diffraction map (e.g., orientation

map or strain map) of the reaction products in nanometer scale (Supplementary Video 2). These can be used as supplementary information to the in situ TEM movies.

Materials

Reagents

- Sulfuric acid (H_2SO_4, 99.99%; Sigma-Aldrich, cat. no. 339741) **! CAUTION** Personal protective equipment must be worn during experiments involving H_2SO_4, because it is a strong acid and can cause skin burns.
- Hydrogen peroxide solution (H_2O_2, 30% (wt/wt) in water; Sigma-Aldrich, cat. no. 216763)
- Double-sided, polished silicon wafer (200 ± 10-μm thick, here 200 ± 10 indicates mean ± s.d., 4-inch diameter; Virginia Semiconductor, part no. 418d1911764)
- Photoresists (MicroResist, cat. no. MA-P-1215)
- Dummy silicon wafer (200 ± 10-μm thick, here 200 ± 10 indicates mean ± s.d., 4-inch diameter; Virginia Semiconductor, part no. 418d2012047-1)
- Hexamethyldisilazane (HMDS, ≥99.99%; Sigma-Aldrich, cat. no. 440191) **! CAUTION** Personal protective equipment must be worn to avoid inhalation and contact, because HMDS has reproductive toxicity. Use with caution. HMDS is flammable; therefore, attention should be paid to avoid sparks during storage and use.
- Developer (Micro Resist Technology, cat. no. MA-D331)
- Acetone (Anaqua Global International, cat. no. TAE11Y1708TH)
- Potassium hydroxide (KOH; Bay Carbon, cat. no. 43319)
- Hydrochloric acid (HCI; Sigma-Aldrich, cat. no. 109072) **! CAUTION** Personal protective equipment must be worn during experiments involving HCl, because it is a strong acid and can cause skin burns.
- Deionized water (DI water, Milli-Q System; Millipore)
- Indium (Aritech Chemazone, cat. no. NCZ-MN-177/20)
- Titanium pellet evaporation materials (Kurt J. Lesker, part no. EVMTI30HXHX)
- Gold pellet evaporation materials (Kurt J. Lesker, part no. EVMAU40QXQ)
- Copper foil (Aritech Chemazone, cat. no. NCZ-MN-177/20)
- Epoxy adhesive (3M, cat. no. MN55144-1000) **! CAUTION** Be careful, because epoxy adhesive may cause an allergic skin reaction. Personal protective equipment (e.g., gloves and goggles) must be worn during experiments involving epoxy adhesive.
- Lithium-ion battery electrolyte (1.0 M $LiPF_6$ in a mixture of EC and DMC solution with a 1:1 volume ratio; Suzhou Duo Duo Chemical Technology, cat. no. LB064)
- Sodium hexafluorophosphate ($NaPF_6$, 98%; Sigma-Aldrich, cat. no. 208051)
- PC (99.7%; Sigma-Aldrich, cat. no. 310328)

Equipment

- Film-thickness measurement system (NanoSpec, model no. 3000)
- Clean sink (Msink16 and Msink18)
- Ultrasonic cleaner (Creworks Equipment, model no. 10L)
- N_2 spray gun (Terra Universal, part no. 2002-24)
- LPCVD furnace (Tystar, model no. Tystar 17)
- Spin coater (Goldwall, part no. CNA 524G)
- Hot plate (Stuart, UC150)
- Prime oven (CAE, model no. YES/LP III–M5)
- Masks for lithography (details in Equipment setup)
- Lithography printer (Neutronix Quintel, model no. Q4000-6)
- Glass Petri dish (120-mm diameter; Huanyu Instrument, model no. JC-18)
- Polytetrafluoroethylene (PTFE) Petri dish (120-mm diameter; LaborXing, cat. no. 4FPYM-120)
- Plasma-thermal parallel plate plasma etcher (Plasma-Therm, model no. PK-12 RIE)
- Vacuum evaporation coater
- Tweezer (Sigma-Aldrich, product no. Z680184)
- Disposable plastic dropper (Kangjian, cat. no. KJ 619)
- Cotton swab (Sigma-Aldrich, product no. WHAWB100035)
- Two cover glasses (VWR International, cat. no. 48382-126)
- Custom support (details in Fig. 5)
- Diaphragm pump (Pfeiffer Vacuum, model no. MVP015-2)

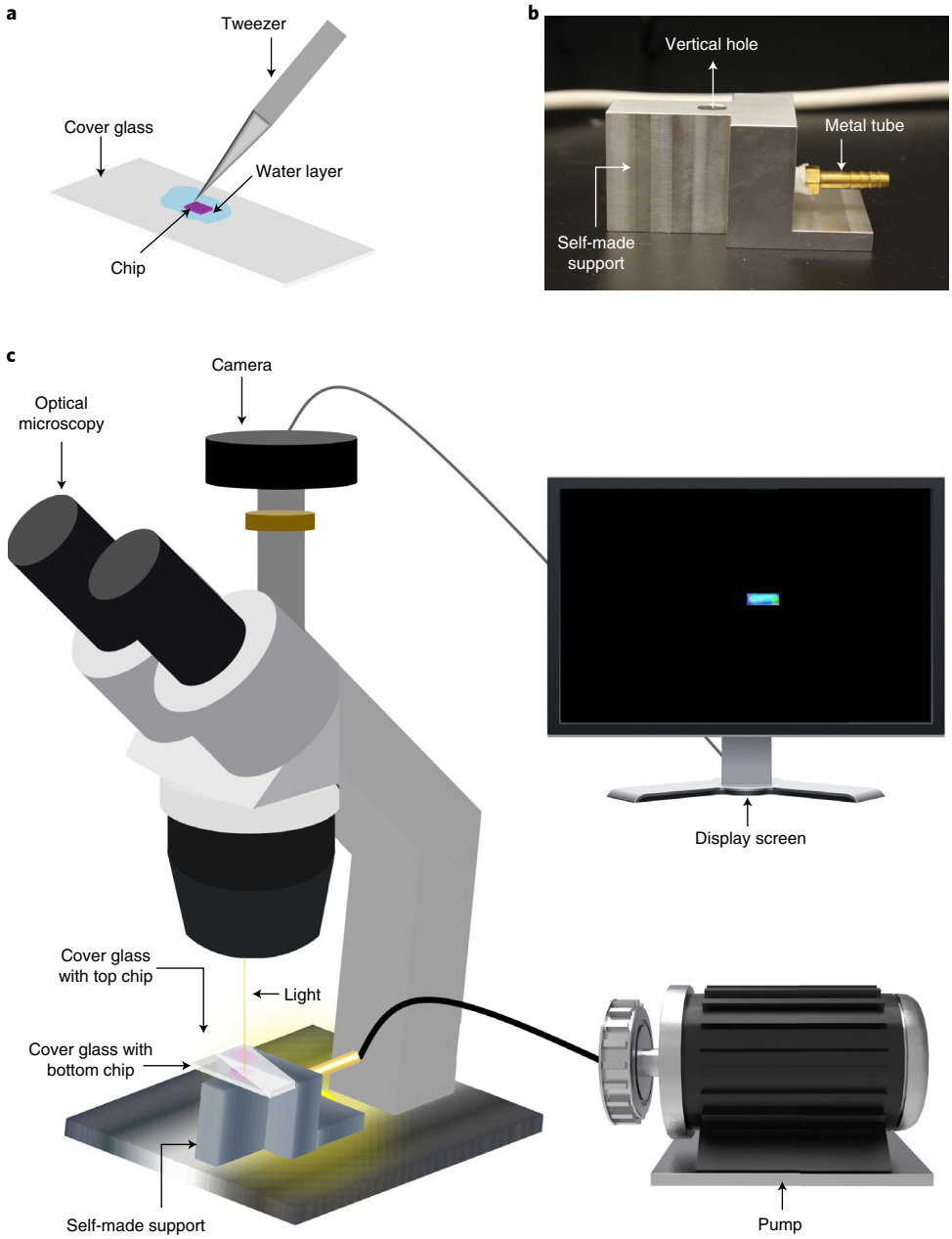

Fig. 5 | Assembly of the top chip and bottom chip. a, Schematic illustration of the operation process for pushing the chip horizontally until it is firmly adsorbed on the surface of the cover glass due to the surface tension of water. **b**, Photograph of the custom support. There is a vertical cylindrical hole (internal diameter: 12 mm) through the support so that the bottom light can travel through the support and cover glasses to the objective lens of optical microscopy, as shown in **c**. There is also a horizontal hole (internal diameter: 6 mm) connecting with the vertical hole in a T shape. This junction cannot be seen in the figure because it is inside the support and covered by the external wall. Another important component here is a metal connecting tube, one end of which is screwed into the horizontal hole of the support, and the other end is connected to the pump, as shown in **c**. This connection allows air to be extracted from the channel in the custom support, fixing the cover glass onto the vertical hole. **c**, Schematic illustration of the alignment process between the top and bottom chips under a microscope.

- Optical microscope (Olympus, model no. SZX16)
- Microscope digital camera (AmScope, model no. MU1000)
- Binder clips (Staples, cat. no. 32003)
- Vacuum drying oven (Kohstar, model no. DZF-6050)
- Wire bonder (West Bond, model no. 7400B)
- Syringe (3 ml, with BD PrecisionGlide 18 G × 1-1/2 inch hypodermic needles, 1.2 mm × 40 mm; BD, cat. no. DG508003)

- PTFE thin-wall tube (with 0.015-inch internal diameter and 0.0159-inch outer diameter, 100 feet/pack; Cole-Parmer Instrument, lot no. 04147138-1)
- PTFE special sub-light-wall tube (with 0.006-inch internal diameter and 0.016-inch outer diameter, 100 feet/pack; Cole-Parmer Instrument, lot no. 01122262-1)
- Soldering station (Weller, cat. no. WES51)
- Electrochemical workstation (CH Instruments, model no. 660D)
- Transmission electron microscope (JEOL, model no. JEOL-2100F)
- High-speed camera (Direct Electron, model no. DE-12)
- Custom TEM holder

Reagent setup

Piranha solution

Piranha solution is a hot mixture of concentrated H_2SO_4 and H_2O_2 solution to remove all organic matter. In this protocol, piranha solution is used in the first step to clean the surface of the silicon wafer. The preparation process of piranha solution is as follows: use a measuring cylinder to measure 70 ml of concentrated H_2SO_4 into a beaker; then, use a measuring cylinder to measure 30 ml of H_2O_2 solution and slowly pour it into a beaker containing concentrated H_2SO_4, stirring it with a glass rod while pouring. **! CAUTION** Personal protective equipment must be worn during experiments involving piranha solution, because it contains strong acids and can cause skin burns. Adding H_2O_2 solution to concentrated H_2SO_4 must be done very slowly, and the adding sequence must not be reversed. The preparation process must be carried out in the fume hood.

Equipment setup

LPCVD setup

The LPCVD process is carried out in a five-zone LPCVD furnace. A schematic of such an LPCVD furnace is provided in Supplementary Fig. 2. In our facility, a formal training course is required to use this piece of equipment. Typically, we use Tystar17 to deposit a 'Low Stress Nitride' film on the wafers, which is a silicon-rich type film. We use the loading recipe 'LSNSTDA', in which the deposition condition is fixed (100 standard cubic centimetres per minute (sccm) dichlorosilane/25 sccm NH_3/140 mTorr/835 °C); for this condition, the deposition rate is ~35 Å/min, and the deposition time is 10 min. For detailed information, see Chapter 5.17 at https://nanolab.berkeley.edu/public/manuals/equipment_manual.shtml.

Lithography

Lithography is performed by using a mask aligner with a UV light source. For detailed information, see Chapter 4.3 or Chapter 4.4 at https://nanolab.berkeley.edu/public/manuals/equipment_manual.shtml. In our facility, a formal training course is required to use this piece of equipment. In this protocol, the contact lithography mode is adopted, during which the aligned mask directly contacts the photoresist film on the wafer. A schematic of such a lithography process is shown in Supplementary Fig. 3a. In each regular mask, there are 1,096 cell units (Supplementary Fig. 3b). Note that, for the preparation of the top chip and bottom chip, the cell units are different. The patterns of the cell unit for the first and second lithography of top chips are shown in Supplementary Fig. 3c and Supplementary Fig. 3d, respectively. The patterns of the cell unit for the first and second lithography of bottom chips are shown in Supplementary Fig. 3e and Supplementary Fig. 3f, respectively.

Plasma etching

The plasma etching process is carried out in a plasma-thermal parallel plate etcher. Typically, we use O_2 = 100 standard cubic centimeters per minute (sccm), power = 250 W for 10 min to clean the chamber; O_2 = 50 sccm, power = 150 W for 1 min to do the descum process; and CHF_3 = 48 sccm, O_2 = 2 sccm, power = 100 W for the SiN*x* etching process. In our facility, a formal training course is required to use this piece of equipment. The basic reaction process in the etching chamber can be divided into five steps: (i) the beginning of the etching process and the generation of plasma etching reaction species, (ii) the diffusion of the reaction species to the surface of the SiN_x film, (iii) the adsorption of the reaction species on the surface of the SiN_x film, (iv) the reaction of the plasma species with SiN_x along with the generation of volatile compounds and (v) the desorption of the generated volatile compounds from the SiN_x surface.

PVD setup

The deposition of the target metal via a PVD process is performed in a high-vacuum thermal evaporation system. This process basically involves three steps: metal gasification, migration and deposition. For the deposition of the indium spacer, we use an NRC evaporator. Typically, we load seven or eight indium pellets in the heating boat, after which, the vacuum pressure is pumped down to ~2×10^{-6} Torr. The specific deposition parameters for indium are as follows: eensity = 7.3, Z ratio = 0.841, tooling = 50. After setting up the parameters, the deposition rate is controlled to be 1 Å/s by tuning the current, and the crystal monitor is used to measure the evaporation (deposition) rate. For the deposition of the titanium electrode, we use an Ultek2 Angled Cooled Chuck E-Beam evaporator. Typically, we load seven or eight titanium pellets in the boat, after which, the vacuum pressure is pumped down to ~5×10^{-6} Torr. The specific deposition parameters for titanium are as follows: density = 4.5, Z ratio = 0.628. After setting up the parameters, the deposition rate is controlled to be 1 Å/s by increasing the current step by step, making sure that the electron beam is in the center of the boat, and the crystal monitor is used to measure the evaporation (deposition) rate. For detailed information, see Chapters 6.35 and 6.37 at https://nanolab.berkeley.edu/public/manuals/equipment_manual.shtml. In our facility, a formal training course is reuired to use this piece of equipment.

Procedure

▲ **CRITICAL** The fabrication procedure (Steps 1–42) applies to both the top and bottom chips. We recommend that the manufacturer prepare one type of chip first and then repeat Steps 1–42 to prepare the other. Of note, the fabrication procedure of the two types of chips is basically the same, with only a few differences. These differences are detailed in the specific steps (Steps 13, 35 and 38) below.

Substrate preparation ● Timing 2 h

Pre-furnace cleaning of the silicon wafer ● Timing 35 min

▲ **CRITICAL** Schematics in Figs. 3a and 4a show the silicon wafer after pre-furnace cleaning.

1 For fabrication of both the top and bottom chips, put the silicon wafer (4 inches, 200 μm) into a clean sink with piranha solution and soak for 10 min.
! CAUTION Personal protective equipment must be worn, because piranha solution contains strong acids and can cause skin burns.

2 After the soaking treatment, put the soaked silicon wafer into DI water and sonicate in an ultrasonic cleaner for four cycles of 5 min.

3 Blow the washed silicon wafer with a N_2 spray gun until it is totally dried.

Low-stress SiN_x growth on the surfaces of the silicon wafer ● Timing 80 min

▲ **CRITICAL** Schematics in Figs. 3b and 4b show the silicon wafer after low-stress SiN_x growth.

4 Uniformly grow the SiN_x on the surfaces of the obtained clean silicon wafer via an LPCVD method in the five-zone LPCVD furnace. For the overall operation information, see Chapter 5.17 at https://nanolab.berkeley.edu/public/manuals/equipment_manual.shtml.

5 After deposition, use a film-thickness measurement system to check the thickness of SiN_x (Supplementary Fig. 4). The typical operating procedure includes the following: placing both the reference wafer and the sample to be measured on the stage; doing a reference calibration; and after the reference calibration, using the tool to test the samples. For the overall operation information, see Chapter 8.24 at https://nanolab.berkeley.edu/public/manuals/equipment_manual.shtml.
▲ **CRITICAL STEP** The thickness of the grown SiN_x is critical and needs to be kept at 35 nm.

Bonding the SiN_x/silicon wafer and dummy wafer ● Timing 5 min

▲ **CRITICAL** Schematics in Figs. 3c and 4c show the wafer after bonding the SiN_x/silicon wafer on the dummy wafer.

6 Drop 2.5-ml photoresists on the surface of the dummy wafer and uniformly apply them by using a spin coater at 2,000 rpm for 45 s.

7 Put the prepared SiN_x/silicon wafer on the photoresist surface of the dummy wafer as quickly as possible. During this process, use your hands to align the SiN_x/silicon wafer and dummy wafer and use a N_2 gun to blow them together gently.

8 Place the bonded wafer on the hot plate manually and bake it at 100 °C for 2 min.
▲ CRITICAL STEP The purpose of baking is to improve the photoresist adhesion and thereby make the SiN_x/silicon wafer bond more firmly to the dummy wafer.

The first lithography ● Timing 1 h

First primer coating ● Timing 45 min

! CAUTION Personal protective equipment must be worn to avoid inhalation and contact, because the primer (HMDS) has reproductive toxicity. Use with caution. HMDS is flammable; therefore, attention should be paid to avoiding sparks during storage and use.

▲ CRITICAL Schematics in Figs. 3d and 4d show the wafer after the first primer coating.

9 Coat the SiN_x surface with HMDS by using the HMDS pretreatment system in a prime oven. For the overall operation information, see Chapter 4.31 at https://nanolab.berkeley.edu/public/manuals/equipment_manual.shtml.
▲ CRITICAL STEP The purpose of primer coating is to remove the moisture on the wafer surface, improve the hydrophobicity of the wafer surface and facilitate the subsequent photoresist coating process.

10 After coating, take out the HMDS-coated wafer with gloves and cool it down for 15 min for the next step.

First photoresist coating ● Timing 5 min

▲ CRITICAL Schematics in Figs. 3e and 4e show the wafer after the first photoresist coating.

11 Drop a 2.5-ml photoresist on the HMDS surface of the HMDS-coated wafer and uniformly apply by using a spin coater at 3,000 rpm for 45 s.

12 Place the wafer on a hot plate and bake it at 100 °C for 2 min. Then, cool it down for 2 min before proceeding to the next step.
▲ CRITICAL STEP The purpose of this soft baking operation is to evaporate the remaining solvent in the photoresist, make the coated photoresist thinner and improve the photoresist adhesion.

First UV exposure ● Timing 5 min

▲ CRITICAL Schematics in Figs. 3f and 4f show the wafer after the first UV exposure.

13 Before UV exposure, align the *y*-axis on the mask with the flat edge on the wafer at 90° with the help of a binocular microscope. The patterns of the cell units for the preparation of top and bottom chips are shown in Supplementary Fig. 3c and e, respectively.
▲ CRITICAL STEP For the preparation of the top chip and bottom chip, the cell units of the mask are different.

14 Expose the wafer under the lithography printer and perform contact line lithography at 200 J/cm^2 for 6.0 s.

15 After exposure, place the wafer on a hot plate and bake it at 100 °C for 2 min. Then, cool it down for 2 min for the next step.
▲ CRITICAL STEP The purpose of baking is to improve the photoresist profile.

First photoresist development ● Timing 5 min

▲ CRITICAL Schematics in Figs. 3g and 4g show the wafer after the first photoresist development.

16 Place the wafer into photoresist developer solution and soak for 30 s.

17 After developing, rinse the wafer by using DI water and air dry.

Etching ● Timing 54 h

Plasma etching ● Timing 0.5 h

▲ CRITICAL Schematics in Figs. 3h and 4h show the wafer after plasma etching.

18 To clean the chamber, start the plasma-thermal parallel plate etcher and set the parameters to: power = 250 W, O_2 = 100 sccm, time = 10 min.

19 Open the chamber and place the wafer on the electrostatic chuck.

20 To descum, close the chamber and set the parameters to: power = 150 W, O_2 = 50 sccm, time = 1 min.

21 After descumming, etch SiN_x by setting the parameters to: power = 100 W, CHF_3 = 48 sccm, O_2 = 2 sccm, time = 1.5 min.

22 After etching, purge the chamber with N_2 to remove CHF_3 and cool the wafer.
! CAUTION CHF_3 is toxic; therefore, before opening the chamber, N_2 purging is critical. If the chamber is hot, pump down for a longer time before opening the chamber, because the wafer is easily broken by the temperature difference.
23 Open the chamber and take out the etched wafer for the next-step treatment.

First liftoff ● Timing 48 h
▲ CRITICAL Schematics in Figs. 3i and 4i show the wafer after first liftoff.
▲ CRITICAL Extreme care is needed, because surface tension may break the wafer while taking it out of the solution.
24 Put the wafer in a glass Petri dish with acetone solution at room temperature (25 ± 1 °C, mean ± s.d.) and soak it for 48 h. The purpose of this step is to remove the photoresist on the wafer and thereby separate the silicon/SiN_x wafer from the dummy wafer.
25 After the silicon/SiN_x wafer is separated from the dummy, rinse the silicon/SiN_x wafer with lots of acetone by using a wash bottle.
26 Blow the rinsed silicon/SiN_x wafer with a N_2 spray gun until the wafer is totally dried and ready for the next step.

Wet etching ● Timing 5.5 h
▲ CRITICAL Schematics in Figs. 3j and 4j show the wafer after wet etching.
▲ CRITICAL Extreme care is needed, because surface tension may break the wafer while taking it out of solution.
27 Put the wafer in 33.3% (wt/wt) KOH solution in a PTFE Petri dish and then soak it in an 80 °C water bath for ~3 h, controlling the temperature by a thermocouple with the tip immersed in the water bath. The purpose of this step is to etch the 200-μm silicon wafer for the imaging window.
▲ CRITICAL STEP This step needs extreme care. After 2 h, check once every 15 min to avoid under-etching and over-etching. In theory, the etching rate of the silicon wafer is 1 μm/min.
28 After etching, gently remove the wafer from the KOH solution and immediately put it into the cleaning solution (H_2O_2/HCl/H_2O = 1:3:5 (vol/vol)) and soak it at room temperature for >2.0 h. The purpose of this step is to remove the residue metal particles or ions.
29 Gently take the wafer out from the cleaning solution and put it in a glass Petri dish filled with DI water.
30 Gently wash the obtained wafer by using large amount of DI water and blow the wafer with a N_2 spray gun with the blowing direction in parallel with the wafer plane.
? TROUBLESHOOTING
31 Put the wafer in a glass Petri dish and cover it to avoid contamination from air dust until the next step.

The second lithography ● Timing 1 h

Flip-over and bonding ● Timing 5 min
▲ CRITICAL Schematics in Figs. 3k and 4k show the wafer after flip-over and bonding.
32 Flip over the patterned silicon/SiN_x wafer and repeat Steps 6–8 to bond the patterned silicon/SiN_x wafer with a dummy wafer.

Second primer coating ● Timing 45 min
▲ CRITICAL Schematics in Figs. 3l and 4l show the wafer after the second primer coating.
33 Repeat Steps 9 and 10 to coat HMDS.

Second photoresist coating ● Timing 5 min
▲ CRITICAL Schematics in Figs. 3m and 4m show the wafer after the second photoresist coating.
34 Repeat Steps 11 and 12 to coat the photoresist.

Second UV exposure ● Timing 5 min
▲ CRITICAL Schematics in Figs. 3n and 4n show the wafer after the second UV exposure.
35 Repeat Steps 13–15 to apply masks on, and UV expose, the wafer. The patterns of the cell units for the preparation of top and bottom chips are shown in Supplementary Fig. 3d and f, respectively.

▲ CRITICAL STEP For the preparation of the top and bottom chips, the cell units of the mask are different.

Second photoresist development ● Timing 5 min

▲ CRITICAL Schematics in Figs. 3o and 4o show the wafer after the second photoresist development.

36 Repeat Steps 16 and 17 for photoresist development.

Metal deposition ● Timing 49 h

Descum ● Timing 20 min

37 Repeat Steps 18–20 for descumming of the wafer.

Metal deposition ● Timing 40 min

▲ CRITICAL Schematics in Figs. 3p and 4p show the wafer after metal deposition.

38 Uniformly deposit the metal (e.g., gold, indium or titanium) on the surface of the obtained wafer via a PVD method (thermal evaporation for gold and indium, electron beam evaporation for titanium) in the vacuum evaporation coater. For the overall operation information, see Chapter 6.35 or 6. 37 at https://nanolab.berkeley.edu/public/manuals/equipment_manual.shtml.

▲ CRITICAL STEP For the preparation of the top and bottom chips, the deposited metals are different: indium deposition is for the top chips, whereas gold (or titanium) deposition is for the bottom chips.

? TROUBLESHOOTING

Second liftoff ● Timing 48 h

▲ CRITICAL Schematics in Figs. 3q and 4q show the obtained bottom chip and top chip.

39 Put the wafer in acetone solution at room temperature and soak it for 48 h. The purpose of this step is to remove the photoresist on the wafer and thereby separate the silicon/SiN_x wafer from the dummy. Metal patterns remain on the wafer after the removal of the photoresist.

40 After separation of the silicon/SiN_x wafer from the dummy, rinse the silicon/SiN_x wafer with lots of acetone (followed by DI water) by using a wash bottle.

? TROUBLESHOOTING

41 Blow the rinsed silicon/SiN_x wafer with a N_2 spray gun, with the blowing direction parallel to the wafer plane, until the chips are totally dried.

? TROUBLESHOOTING

42 Because each silicon wafer will produce hundreds of top or bottom chips, individual chips need to be separated. Use tweezers to poke the wafer-scale chips away from each other, to obtain separated chips (Fig. 4q) ready for the next step.

Assembly ● Timing 1 h

Assembly of the top and bottom chips ● Timing 40 min

▲ CRITICAL Schematics in Figs. 3r and 4r show the liquid cell during assembly of the top and bottom chips.

43 Apply one or two drops of DI water to the center of a cover glass by using a disposable plastic dropper and then use a cotton swab to evenly distribute the drops into a very thin water layer. Repeat with a second cover glass (one will be for the top chip and the second for the bottom chip).

44 Quickly place the top chip (the metal-deposited side faces up) onto the water layer of one cover glass and the bottom chip (the metal-deposited side faces up) on the other and move the chip around in the glass plane by using tweezers until the water layer sticks the chip firmly onto the glass substrate by capillary force or surface tension of water. A schematic of this step is shown in Fig. 5a.

▲ CRITICAL STEP Be careful when fixing the chip on the cover glass, because water can contaminate the chip's window.

45 Place the bottom cover glass (with the bottom chip attached) over the hole in the custom support with the chip facing up. Turn on the pump (which is connected to the tube of the support) to extract air through the channel in the support, fixing the cover glass in position. A schematic of the custom support is shown in Fig. 5b, and a schematic of this step is shown in the bottom part of Fig. 5c.

46 Hold the top cover glass (with the top chip attached) with your hand and move it slowly and horizontally under the optical microscope until a bright rectangle area appears on the computer monitor. Then, with only vertical movement (the chip must not be moved horizontally), move the top glass down until the top chip is fully in contact with the bottom chip. A schematic of this step is

shown in Fig. 5c. Note that, during this process, if the top chip–imaging window (transparent) and bottom chip–imaging window (transparent) are well aligned, the light (emitted from the base of the optical microscope) will go through both the bottom and top imaging windows and hit on the microscope digital camera, and thereby the camera will detect the light and show a bright rectangle area on the computer monitor. Therefore, the appearance of the bright rectangular area on the computer monitor can be used as a sign of successful alignment.

47 After alignment, use two binder clips to clamp the two short sides of the top and bottom cover glass. The purpose of this step is to temporarily fix the aligned top and bottom chips together so that the two aligned chips do not move in subsequent operations.

▲ **CRITICAL STEP** During the process of clamping the clip onto the two cover glasses, any lateral movement of the chip is likely to cause the aligned imaging windows to misalign. Consequently, the electrode cannot be observed in the subsequent TEM observation, resulting in a failed liquid cell. Therefore, this step requires extra care and accuracy to ensure that there is no lateral movement between the two aligned chips.

? TROUBLESHOOTING

48 Put the clamped glass into an oven and heat at 120 °C for 2 h.

49 Take the clamped glass out of the oven and let it cool down to room temperature. Once cooled, the two chips will be bonded together. Note that by heating the chips in the oven, the indium metal will be half melted. After cooling, the indium metal will resolidify, bonding together the two chips.

? TROUBLESHOOTING

50 Evenly coat epoxy all around the sides of the liquid cell (Figs. 3s and 4s). The purpose of this step is to enhance the bonding connection of the top chip and bottom chip, as well as permanently fix the relative horizontal and vertical position of the top chip versus the bottom chip. This will also prevent liquid leakage from the sides.

? TROUBLESHOOTING

Wire bonding ● Timing 5 min

▲ **CRITICAL** Schematics in Figs. 3t and 4t show the liquid cell after wire bonding.

51 Bond the gold (aluminum) wires onto each gold (titanium) pad in two reservoirs by using a wire bonder, operating under an optical microscope. A schematic of this step is shown in Fig. 6a. For detailed information, see Chapter 9.4 at https://nanolab.berkeley.edu/public/manuals/equipment_manual.shtml.

▲ **CRITICAL** The SiN_x membrane is only 35-nm thick, and the reservoir dimension is 700 μm × 500 μm. This leaves a large lateral dimension of SiN_x membrane without silicon substrate support. Consequently, the SiN_x membranes break easily. After several steps of the rinsing and blowing processes, especially after Step 30, most of the reservoir SiN_x membranes (with length × width × thickness = 700 μm × 500 μm × 35 nm) throughout the entire wafer will have broken, although quite a few reservoir membranes will still be intact. However, after the fabrication (Steps 31–50), all the reservoir membranes will be broken, allowing the wires to pass through and be bonded onto a gold (titanium) pad in the two reservoirs.

? TROUBLESHOOTING

Loading electrolyte ● Timing 5 min

▲ **CRITICAL** Schematics in Figs. 3u and 4u show the liquid cell after loading electrolyte.

52 Inject the commercial electrolyte (e.g., 1 M $LiPF_6$ dissolved in 1:1 (vol/vol) EC and DEC) into the reservoir under an optical microscope by using a syringe. The needle end should be equipped with a PTFE thin-wall tube, with another, even smaller PTFE special sub-light-wall tube inserted into its front end (Tubes 1 and 2 in the schematic in Fig. 6b). During this process, the liquid electrolyte will spread out quickly in the entire space of the liquid cell by capillary force. A schematic of this step is shown in Fig. 6b.

▲ **CRITICAL STEP** The purpose of these frontside tubes is to control the flow rate of liquid electrolyte into the reservoir and avoid overflow, because overflow can severely contaminate the SiN_x imaging window on the top side and thus reduce the imaging resolution of the electrochemical liquid cell. Using an optical microscope helps to align the end of the tube with the reservoir, thereby ensuring accurate injection.

? TROUBLESHOOTING

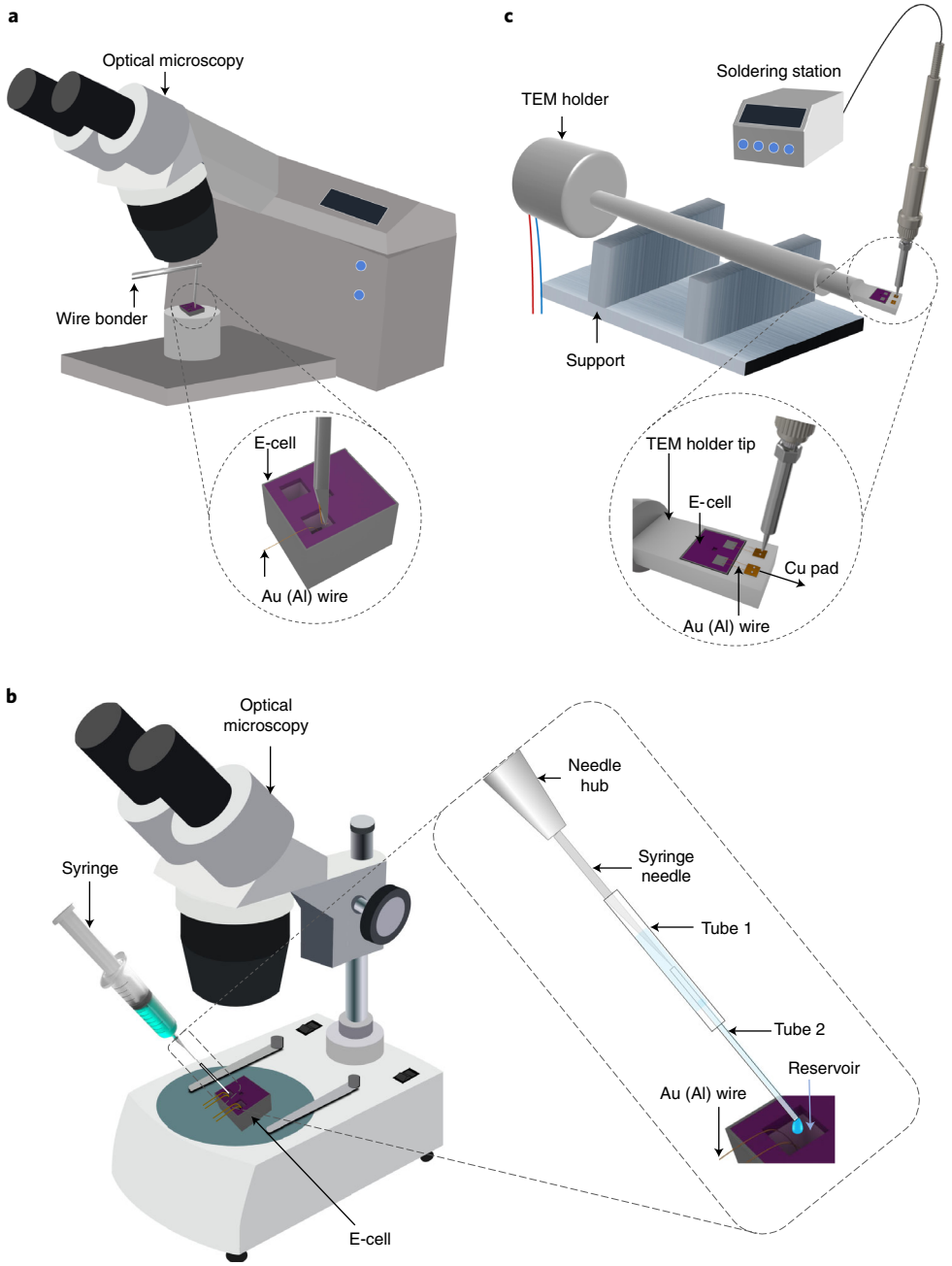

Fig. 6 | Operation process for wire bonding, loading liquid electrolyte and incorporating the prepared E-cell on the TEM holder. a, Schematic illustration of the wire bonding process. Under the optical microscope, a wire bonder is used to bond the gold (aluminum) wires onto each gold (titanium) pad in two reservoirs of the E-cell. **b**, Schematic illustration of electrolyte loading. Under the optical microscope, a syringe is used to inject the electrolyte into the reservoir of the E-cell. Note that the needle end of the syringe is equipped with a PTFE thin-wall tube (Tube 1), with a smaller PTFE special sub-light-wall tube (Tube 2) inserted in its front end. **c**, Schematic illustrating the process of soldering the gold (aluminum) wires from the E-cell on the copper pad of the TEM holder. The soldering station is used to solder the extended gold (aluminum) wires that were bonded onto gold (titanium) pads of the E-cell to the two copper pads of the custom TEM holder tip.

Sealing ● Timing 5 min

53 Cover each of the two reservoirs with a copper foil (Figs. 3v and 4v).

54 Apply epoxy adhesive to the top and around the copper foils for a better seal (Figs. 3w and 4w). **! CAUTION** Be careful, because the epoxy adhesive may cause an allergic skin reaction. Personal protective equipment (e.g., gloves and goggles) must be worn during this step.

55 Put the liquid cell coated with epoxy in a dry place for natural drying and curing. Once dry, the final electrochemistry liquid cell is complete.

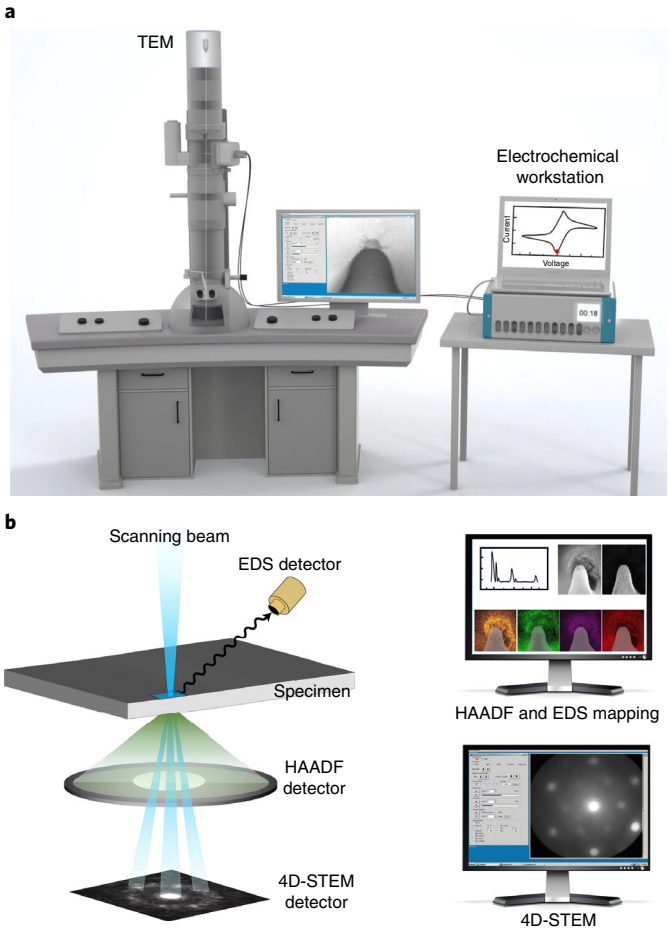

Fig. 7 | Schematic illustration of the in situ TEM observation and post in situ characterizations. a, Setup for in situ TEM observation. **b**, Post in situ characterizations, which include HAADF-STEM, EDS and 4D-STEM techniques. The left half of the panel designates three techniques combined together; each technique uses different detectors to collect the signals. The right half of the panel shows the collected HAADF, EDS mapping and 4D-STEM images.

Incorporating the prepared cell on the TEM holder ● Timing 5 min

56 Place the prepared electrochemistry liquid cell in the cell pocket on the custom TEM holder tip (Supplementary Fig. 5).

57 Then, locate the extended gold (aluminum) wires that were bonded onto the gold (titanium) pads of the electrochemistry liquid cell and, using a soldering station, solder them to the two copper pads of the custom TEM holder tip. A schematic of this step is shown in Fig. 6c.
? TROUBLESHOOTING

TEM observation ● Timing 2 h

58 Insert the TEM holder into the TEM instrument (JEOL 2100 TEM) and connect it to the electrochemical workstation.

59 While operating the TEM equipment for in situ capturing, run a cyclic voltammetry voltage program by using the CHI electrochemical workstation and record the electrochemical reactions on gold (titanium) electrodes in the liquid cell. A schematic of this step is shown in Fig. 7a.

HAADF-STEM, EDS and 4D-STEM characterizations ● Timing 2 h

60 After recording the electrochemical reaction in the liquid cell, conduct HAADF-STEM, EDS and/or 4D-STEM characterizations. Schematics of the HAADF-STEM, EDS and 4D-STEM techniques are shown in Fig. 7b, and more details of 4D-STEM can be found in a previous publication[38].

Troubleshooting

Troubleshooting advice can be found in Table 1.

Table 1 | Troubleshooting table

Step	Problem	Possible reason	Solution
30	SiN_x windows are broken	Washing or blowing the silicon wafer with the water spray or N_2 spray gun perpendicular to the silicon wafer plane	Gently wash or blow the silicon wafer with the water spray or N_2 spray gun in parallel with the wafer plane
38	The thickness of the deposited gold or titanium electrode or indium spacer is far from the designed thickness	The crystal monitor is overused such that it cannot detect the deposited film in the correct way	Replace the crystal monitor with a new one
	The deposited gold or titanium electrode or indium spacer is too rough, so that it will influence the later fabrication or assembly process	The evaporation rates of gold, titanium and indium metals are too high, because of the applied electric current in the program setting being too high	Reduce the applied electric current in the program setting to reduce the thermal evaporation rate of gold and indium metal, and reduce the electron beam evaporation rate of titanium metal
40	Some dark spots appear in the SiN_x window area (when the SiN_x windows are checked by using TEM)	Insufficient acetone flushing on the silicon/SiN_x wafer, so that there are some photoresist residue remains on the SiN_x film	Rinse the silicon/SiN_x wafer by using an acetone (followed by DI water) wash bottle, with a flushing direction in parallel to the wafer plane homogeneously across the whole wafer, repeating the flushing process as many times as possible
41	Some traces of solvent or water stains appear in the SiN_x window area after the drying process	Uneven blowing process throughout the wafer	Quickly blow the silicon wafer in one direction to push the continuous liquid layer from one side to the other side and let the liquid layer eventually fly out from the edge side of the silicon wafer
47	The top chip and bottom chip are initially well aligned by checking both SiN_x windows by using light, but when clips are applied, the window becomes misaligned, such that light cannot pass through both chips in the SiN_x window area	There is a lateral movement when manually applying clips onto both chips	Take extreme care when applying clips to ensure that there is no lateral movement between the top chip and bottom chip
49	The indium metal cannot bond the bottom chip effectively	Insufficient flushing of the silicon/SiN_x wafer in Step 40, so there is some photoresist residue on indium metal	Repeatedly rinse the indium spacer (firstly in acetone, then in DI water) more than 10 times to thoroughly remove the photoresist residue. After that, perform 1 min of O_2 plasma treatment to remove adsorbed acetone molecules
50	The seal around the sides of the liquid cell is not good, so that the cell has some leakage	Deficient coating on the side of the liquid cell because of small holes or gaps that cannot be observed by the naked eye	Use optical microscopy to double-check the coating on the sides of the liquid cell to make sure that there are no holes on either side of the liquid cell
51	The connection between the gold (aluminum) wires and gold (titanium) pad is not good, and the wire easily breaks from the pad	The ultrasonic power for the wire bonder is too high, such that it excessively melts the gold (aluminum) wire on the gold (titanium) pad, leading to the connection point being too thin to break	Reduce the ultrasonic power or cut down the time of ultrasonic heating Wire bond three gold (aluminum) wires onto the gold (titanium) pad to guarantee that there are a sufficient number of wires forming a connection
52	Large droplets overflow from the reservoir and contaminate the SiN_x imaging window on the top side	The pressure in the syringe is too high, pushing excess liquid into large droplets at the bottom tip of the PTFE sub-light-wall Tube 2 (Fig. 6b)	Adjust the droplet size by using absorbent paper to absorb the liquid droplet until the droplet forms a suitable size (volume) to load into the reservoir and avoid overflow
57	The bonding or contact between the melted tin metal droplet (solder) and copper pad (on the TEM holder tip) is not good during soldering, leading to insufficient voltage program transfer from the electrochemical working station to the electrochemical liquid cell	The copper pad is passivated, or its surface is not clean	Clean and polish the copper pad on the TEM holder tip to make sure that there is good conductivity for the copper pad

Timing

Steps 1–8, substrate preparation: 2 h
Steps 9–17, lithography: 1 h
Steps 18–31, etching: 54 h
Steps 32–36, second lithography: 1 h
Steps 37–42, metal deposition: 49 h
Steps 43–57, assembly: 1 h
Steps 58–59, TEM observation: 2 h
Step 60, HAADF-STEM, EDS and 4D-STEM characterizations: 2 h

Training a competent graduate student or postdoc to master the whole protocol takes ~30 d (8 h/d). Training a lithography engineer to master the whole protocol can reduce training time to 15 d (8 h/d).

Anticipated results

Liquid cell fabrication

After the sealing step (Step 55), the final electrochemical liquid cell (3 mm × 3 mm) is completed (Fig. 1a). Note that, by adjusting the types of the deposited electrodes (Step 38) and the encapsulated liquid electrolytes (Step 52), a series of structurally similar but functionally diverse cells can be synthesized (cells I–III in Table 2). However, throughout the procedure, improper execution of some steps (as highlighted in the Troubleshooting section, Table 1) will result in the failure of the fabricated electrochemical liquid cell. In our experience, the typical yield of the final product has an ~60% success rate.

TEM observation

The fabricated electrochemical liquid cell I (gold electrode, commercial $LiPF_6$/EC/DEC electrolyte) is used for the direct visualization of lithiation and delithiation of the gold electrode (Fig. 8). Electrolyte

Table 2 | Electrochemical liquid cells fabricated by this protocol

Cell	Electrode	Electrolyte	Application
I	Gold	$LiPF_6$/EC/DEC	In situ observation of lithium dendritic growth and the lithiation and delithiation of the gold electrode
II	Titanium	$LiPF_6$/EC/DEC	In situ observation of the lithiation and delithiation of MoS_2 nanosheets
III	Titanium	$NaPF_6$/PC	In situ observation of sodium metal deposition

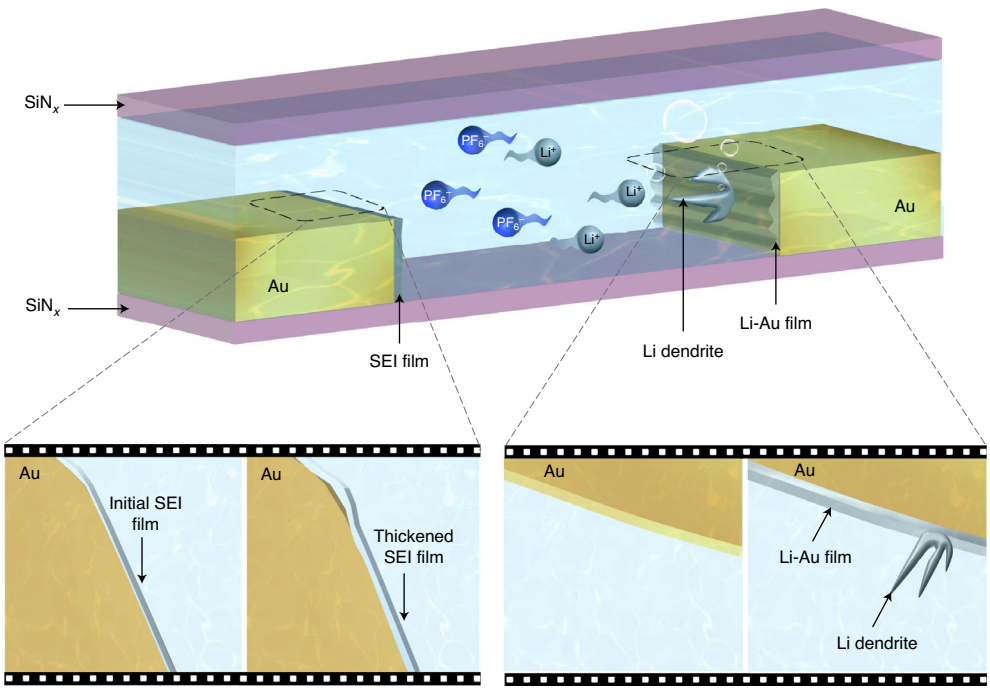

Fig. 8 | In situ TEM observation of the lithium-gold reaction using E-cell I (gold electrode, commercial $LiPF_6$/EC/DEC electrolyte). Top: section view of E-cell I at the imaging window, showing the internal environment of E-cell I and the SEI film growth, lithium-gold film formation and the growth of lithium metal dendrites. Bottom: schematic illustration of SEI film growth, lithium-gold film formation and the growth of lithium metal dendrites. For the original TEM video, see ref. [22].

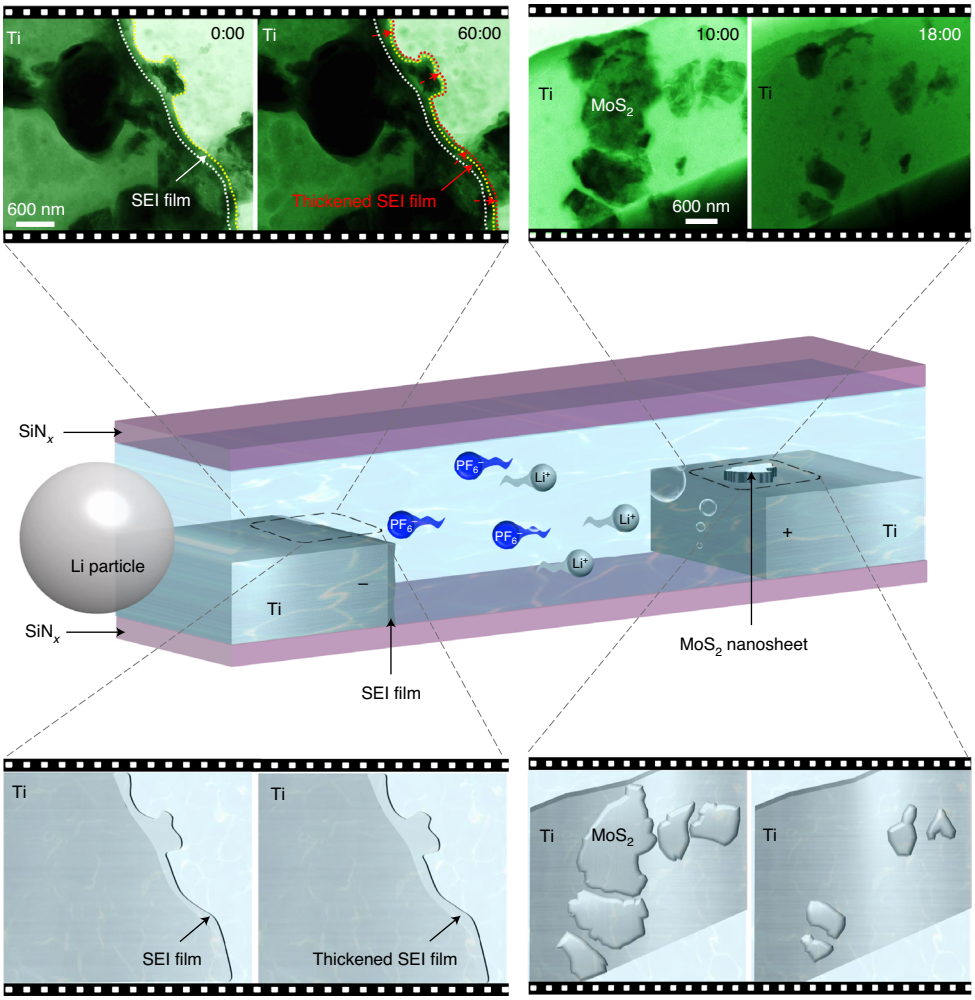

Fig. 9 | In situ TEM observation of the lithiation and delithiation of MoS_2 nanosheets by using E-cell II (titanium/MoS_2 electrode, commercial $LiPF_6$/EC/DEC electrolyte). Top: sequential TEM images from Supplementary Videos 3 and 4, showing the SEI growth and MoS_2 decomposition process. Color is used to guide the eyes. Bottom: schematic illustration of SEI growth and MoS_2 decomposition process. Middle: section view of the E-cell at the imaging window, showing the internal environment of E-cell II and the SEI growth and MoS_2 decomposition phenomenon. The TEM images (top row) adapted with permission from ref. [23], American Chemical Society.

decomposition, lithiation of gold, lithium-gold film formation and the growth and dissolution of lithium metal dendrites are observed in turn. The fabricated electrochemical liquid cell II (titanium/MoS_2 electrode, commercial $LiPF_6$/EC/DEC electrolyte) is used to observe the lithiation and delithiation of MoS_2 nanosheets (Fig. 9 and Supplementary Videos 3 and 4). Real-time TEM images reveal the irreversible decomposition of MoS_2 nanosheets into 5–10-nm MoS_2 nanoparticles. Note that the MoS_2 nanosheets mentioned here are layered onto one of the titanium electrodes during fabrication. Specifically, before loading the electrolyte (Step 52), a droplet of a dispersion containing MoS_2 nanosheets is loaded into one reservoir of the electrochemical liquid cell in the same way as loading electrolyte. Electrochemical liquid cell III (titanium electrode, commercial $NaPF_6$/PC electrolyte) is applied for the direct visualization of sodium metal deposition on the titanium electrodes with different surface roughness (e.g., flat (Fig. 10, Supplementary Fig. 6 and Supplementary Video 5) or sharp curvature (Supplementary Fig. 7 and Supplementary Video 6)). Real-time movies and sequential images show that relatively large sodiu grains (in the micrometer scale) are deposited on the flat titanium electrode surface, whereas small sodium grains (in tens of nanometers) grow explosively on the titanium electrode with undulant surfaces. In addition, comparative analysis of bubble formation from electrolyte decomposition in electrochemical liquid cells I and II is also performed (Supplementary Fig. 8), which demonstrates the gold-catalyzed bubble formation from electrolyte decomposition.

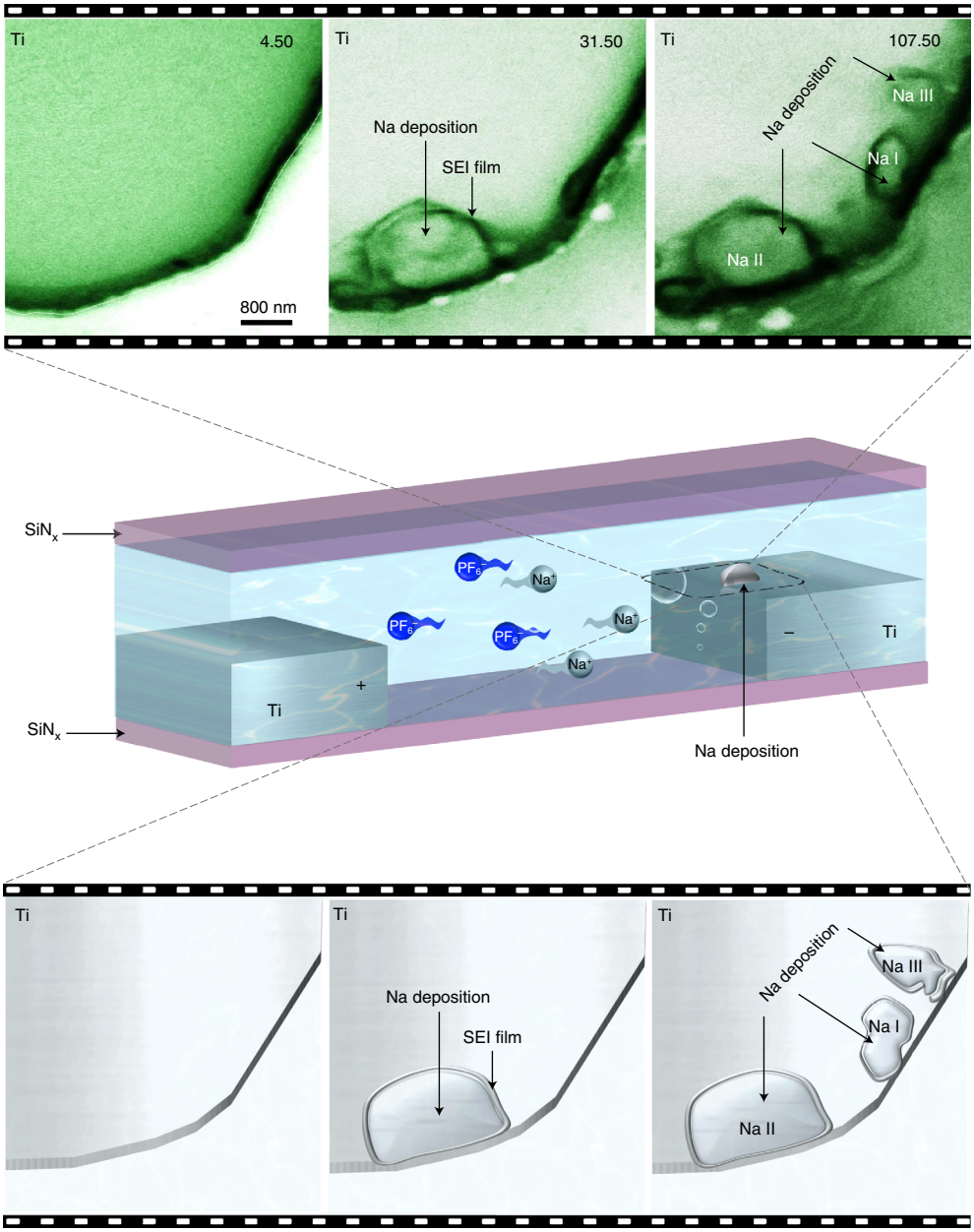

Fig. 10 | In situ TEM observation of sodium electrodeposition on a flat titanium surface by using E-cell III (titanium electrode, commercial $NaPF_6$/PC electrolyte). Top: sequential TEM images from Supplementary Video 5, showing sodium metal deposition on the titanium electrodes with flat surface. Color is used to guide the eyes. Bottom: schematic illustration of sodium electrodeposition on the flat titanium surface. Middle: the section view of the E-cell at the imaging window, showing the internal environment of the E-cell III and the sodium metal deposition phenomenon. The TEM images (top row) adapted with permission from ref. [25], Elsevier.

HAADF, EDS and 4D-STEM characterizations

After the electrochemical reaction in electrochemical liquid cell II (titanium/MoS_2 electrode, commercial $LiPF_6$/EC/DEC electrolyte) is stopped, the structural and compositional information of the SEI film formed on the titanium anode is probed by HAADF, EDS and 4D-STEM characterizations. The anticipated results are shown in Fig. 11, which reveal that the SEI layer contains C, O and F species, with LiF nanocrystals evenly distributed in the whole SEI layer.

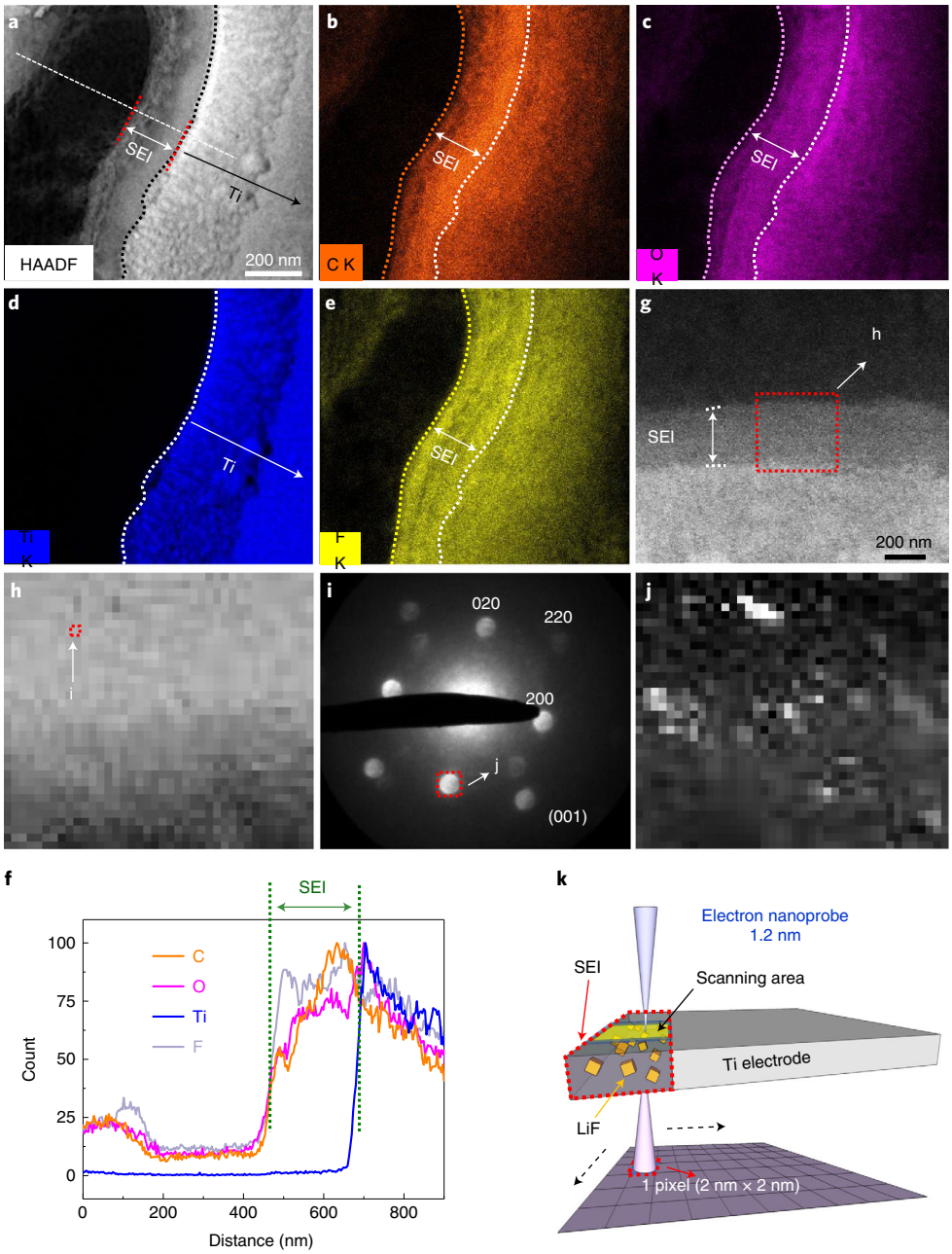

Fig. 11 | Characterization of the SEI layer on the titanium anode in E-cell II (titanium/MoS_2 electrode, commercial $LiPF_6$/EC/DEC electrolyte). **a**, HAADF image. **b–e**, EDS mapping of C, O, Ti and F elements. **f**, EDS line scan marked in **a**. **g**, HAADF image of the SEI layer. The red dashed box is the nanobeam diffraction acquiring area. **h**, Reconstructed BF image obtained from the diffraction series. **i**, Reconstructed virtual diffraction patterns selected from regions marked 'i' in **h**. **j**, Virtual dark-field image reconstructed by using the selected single diffraction spot in **i**. **k**, A schematic showing the nanobeam diffraction characterization of the SEI layer. Figure adapted with permission from ref. [23], American Chemical Society.

Data availability

The main data supporting the findings of this study were previously published in the supporting primary research papers. Additional imaging data are in the Supplementary Figures or are available from the corresponding author upon reasonable request.

References

1. Spurgeon, S. R. et al. Towards data-driven next-generation transmission electron microscopy. *Nat. Mater.* **20**, 274–279 (2021).
2. de Jonge, N., Houben, L., Dunin-Borkowski, R. E. & Ross, F. M. Resolution and aberration correction in liquid cell transmission electron microscopy. *Nat. Rev. Mater.* **4**, 61–78 (2019).

3. Nellist, P. D. et al. Direct sub-angstrom imaging of a crystal lattice. *Science* **305**, 1741 (2004).
4. Yang, R. et al. High-yield production of mono- or few-layer transition metal dichalcogenide nanosheets by an electrochemical lithium ion intercalation-based exfoliation method. *Nat. Protoc.* **17**, 358–377 (2022).
5. Yang, R. et al. MnO_2-based materials for environmental applications. *Adv. Mater.* **33**, e2004862 (2021).
6. Ross Frances, M. Opportunities and challenges in liquid cell electron microscopy. *Science* **350**, aaa9886 (2015).
7. de Jonge, N. & Ross, F. M. Electron microscopy of specimens in liquid. *Nat. Nanotechnol.* **6**, 695–704 (2011).
8. De Yoreo, J. J. & Sommerdijk, N. A. J. M. Investigating materials formation with liquid-phase and cryogenic TEM. *Nat. Rev. Mater.* **1**, 16035 (2016).
9. Kashin, A. S. & Ananikov, V. P. Monitoring chemical reactions in liquid media using electron microscopy. *Nat. Rev. Chem.* **3**, 624–637 (2019).
10. Zeng, Z., Zheng, W. & Zheng, H. Visualization of colloidal nanocrystal formation and electrode–electrolyte interfaces in liquids using TEM. *Acc. Chem. Res.* **50**, 1808–1817 (2017).
11. Zheng, H., Meng, Y. S. & Zhu, Y. Frontiers of in situ electron microscopy. *MRS Bull.* **40**, 12–18 (2015).
12. Zheng, H. et al. Observation of single colloidal platinum nanocrystal growth trajectories. *Science* **324**, 1309–1312 (2009).
13. Yuk Jong, M. et al. High-resolution EM of colloidal nanocrystal growth using graphene liquid cells. *Science* **336**, 61–64 (2012).
14. Liao, H.-G., Cui, L., Whitelam, S. & Zheng, H. Real-time imaging of Pt_3Fe nanorod growth in solution. *Science* **336**, 1011–1014 (2012).
15. Liao, H.-G. et al. Facet development during platinum nanocube growth. *Science* **345**, 916–919 (2014).
16. Yang, J. et al. Formation of two-dimensional transition metal oxide nanosheets with nanoparticles as intermediates. *Nat. Mater.* **18**, 970–976 (2019).
17. Li, D. et al. Direction-specific interactions control crystal growth by oriented attachment. *Science* **336**, 1014–1018 (2012).
18. Nielsen, M. H., Aloni, S. & De Yoreo, J. J. In situ TEM imaging of $CaCO_3$ nucleation reveals coexistence of direct and indirect pathways. *Science* **345**, 1158–1162 (2014).
19. Smeets, P. J. M., Cho, K. R., Kempen, R. G. E., Sommerdijk, N. A. J. M. & De Yoreo, J. J. Calcium carbonate nucleation driven by ion binding in a biomimetic matrix revealed by in situ electron microscopy. *Nat. Mater.* **14**, 394–399 (2015).
20. Williamson, M. J., Tromp, R. M., Vereecken, P. M., Hull, R. & Ross, F. M. Dynamic microscopy of nanoscale cluster growth at the solid–liquid interface. *Nat. Mater.* **2**, 532–536 (2003).
21. Huang, J. Y. et al. In situ observation of the electrochemical lithiation of a single SnO_2 nanowire electrode. *Science* **330**, 1515–1520 (2010).
22. Zeng, Z. et al. Visualization of electrode–electrolyte interfaces in $LiPF_6$/EC/DEC electrolyte for lithium ion batteries via in situ TEM. *Nano Lett.* **14**, 1745–1750 (2014).
23. Zeng, Z. et al. In situ study of lithiation and delithiation of MoS_2 nanosheets using electrochemical liquid cell transmission electron microscopy. *Nano Lett.* **15**, 5214–5220 (2015).
24. Zeng, Z., Liang, W.-I., Chu, Y.-H. & Zheng, H. In situ TEM study of the Li–Au reaction in an electrochemical liquid cell. *Faraday Discuss.* **176**, 95–107 (2014).
25. Zeng, Z. et al. Electrode roughness dependent electrodeposition of sodium at the nanoscale. *Nano Energy* **72**, 104721 (2020).
26. Zhang, Q. et al. In situ TEM visualization of LiF nanosheet formation on the cathode-electrolyte interphase (CEI) in liquid-electrolyte lithium-ion batteries. *Matter* **5**, 1235–1250 (2022).
27. Yuan, Y., Amine, K., Lu, J. & Shahbazian-Yassar, R. Understanding materials challenges for rechargeable ion batteries with in situ transmission electron microscopy. *Nat. Commun.* **8**, 15806 (2017).
28. Fan, Z. et al. In situ transmission electron microscopy for energy materials and devices. *Adv. Mater.* **31**, e1900608 (2019).
29. Kushima, A. et al. Charging/discharging nanomorphology asymmetry and rate-dependent capacity degradation in Li–oxygen battery. *Nano Lett.* **15**, 8260–8265 (2015).
30. Kushima, A. et al. Liquid cell transmission electron microscopy observation of lithium metal growth and dissolution: root growth, dead lithium and lithium flotsams. *Nano Energy* **32**, 271–279 (2017).
31. Beermann, V. et al. Real-time imaging of activation and degradation of carbon supported octahedral Pt–Ni alloy fuel cell catalysts at the nanoscale using in situ electrochemical liquid cell STEM. *Energy Environ. Sci.* **12**, 2476–2485 (2019).
32. Kühne, M. et al. Reversible superdense ordering of lithium between two graphene sheets. *Nature* **564**, 234–239 (2018).
33. Lee, S.-Y. et al. Unveiling the mechanisms of lithium dendrite suppression by cationic polymer film induced solid–electrolyte interphase modification. *Energy Environ. Sci.* **13**, 1832–1842 (2020).
34. De Jonge, N., Peckys, D. B., Kremers, G. & Piston, D. Electron microscopy of whole cells in liquid with nanometer resolution. *Proc. Natl Acad. Sci. USA* **106**, 2159–2164 (2009).
35. Peckys, D. B. & de Jonge, N. Visualizing gold nanoparticle uptake in live cells with liquid scanning transmission electron microscopy. *Nano Lett.* **11**, 1733–1738 (2011).
36. Lu, Y. et al. Self-hydrogenated shell promoting photocatalytic H_2 evolution on anatase TiO_2. *Nat. Commun.* **9**, 2752 (2018).

37. Yuk, J. M., Seo, H. K., Choi, J. W. & Lee, J. Y. Anisotropic lithiation onset in silicon nanoparticle anode revealed by in situ graphene liquid cell electron microscopy. *ACS Nano* **8**, 7478–7485 (2014).
38. Gammer, C., Burak Ozdol, V., Liebscher, C. H. & Minor, A. M. Diffraction contrast imaging using virtual apertures. *Ultramicroscopy* **155**, 1–10 (2015).

Acknowledgements
Z.Z. acknowledges the ECS scheme (CityU9048163) from RGC in Hong Kong and Basic Research Project from Shenzhen Science and Technology Innovation Committee in Shenzhen, China (No. JCYJ20210324134012034).

Author contributions
Z.Z. developed the protocol and performed the experiments. R.Y., J.L. and Z.Z. drafted and envisioned the manuscript. L.M., Y.F., Q.Z., H.-G.L. and J.Y. provided some comments on the manuscript. All authors reviewed the manuscript.

Competing interests
The authors declare no competing interests.

Additional information
Supplementary information The online version contains supplementary material available at https://doi.org/10.1038/s41596-022-00762-y.

Correspondence and requests for materials should be addressed to Ju Li or Zhiyuan Zeng.

Peer review information *Nature Protocols* thanks Nicholas Clark and the other, anonymous, reviewer(s) for their contribution to the peer review of this work.

Reprints and permissions information is available at www.nature.com/reprints.

Publisher's note Springer Nature remains neutral with regard to jurisdictional claims in published maps and institutional affiliations.

Received: 17 December 2021; Accepted: 12 July 2022;
Published online: 04 November 2022

Related links
Key references using this protocol
Zhang, Q. et al. *Matter* **5**, 1235–1250 (2022): https://doi.org/10.1016/j.matt.2022.01.015
Zeng, Z. et al. *Nano Energy* **72**, 104721 (2020): https://doi.org/10.1016/j.nanoen.2020.104721
Zeng, Z. et al. *Nano Lett.* **15**, 5214–5220 (2015): https://doi.org/10.1021/acs.nanolett.5b02483
Zeng, Z. et al. *Faraday Discuss.* **176**, 95–107 (2014): https://doi.org/10.1039/C4FD00145A

Key data used in this protocol
Zeng, Z. et al. *Nano Lett.* **14**, 1745–1750 (2014): https://doi.org/10.1021/nl403922u